J Math Chem (2008) 44:787–801
DOI 10.1007/s10910-007-9341-8

# Pseudospectral methods of solution of the Schrödinger equation

**Joseph Q. W. Lo · Bernie D. Shizgal**

Received: 23 October 2007 / Accepted: 23 November 2007 / Published online: 13 February 2008


**Abstract** Several different pseudospectral methods of solution of the Schrödinger equation are applied to the calculation of the eigenvalues of the Morse potential for $I_2$ and the Cahill–Parsegian potential for $Ar_2$ [Cahill, Parsegian, J. Chem. Phys. **121**, 10839 (2004)]. The calculation of the eigenvalues for the Woods–Saxon potential are also considered. The convergence of the eigenvalues with a quadrature discretization method is found to be very fast owing to the judicious choice for the weight function, basis set and quadrature points. The weight function used is either related to the exact ground state wavefunction, if known, or an approximation to it from some reference potential. We compare several different pseudospectral methods.

**Keywords** Pseudospectral · Schroedinger equation · Morse potential · Woods–Saxon potential

## 1 Introduction

There has been an ongoing effort by numerous researchers to develop accurate and efficient algorithms for the calculation of the eigenvalues of the one dimensional

J. Q. W. Lo (✉)
Institute of Applied Mathematics, University of British Columbia, Vancouver, BC, Canada V6T 1Z1
e-mail: qwlo@iam.ubc.ca

B. D. Shizgal
Laboratoire Diendonné, Université Nice-Sophia Antipolis, Campus Valrose, Nice, France
e-mail: shizgal@theory.chem.ubc.ca
URL: http://www.chem.ubc.ca/personnel/faculty/shizgal/

*Present Address:*
B. D. Shizgal
Department of Chemistry, University of British Columbia, 2036 Main Mall, Vancouver, BC, Canada V6T 1Z1

Schrödinger equation for several different potentials. Although these one dimensional calculations are not computationally intensive, their improvement will find useful application to multidimensional problems. Examples of this research endeavor are the papers by Simos and coworkers that are concerned with either higher order algebraic methods [1], and direct integrations with a Numerov [2], Runge-Kutta [3,4] or symplectic methods [5,6]. Other methods include a Ricatti-Pade approach [7], a Chebyshev–Lanczos method [8] and a Hill determinant method [9] to mention just a few. Other references to similar studies were provided in previous papers [10,11]. Pseudospectral methods include the quadrature discretization method [10,12,13], the discrete variable representation [14], and the Lagrange mesh method [15–17]. Other pseudospectral methods based on classical bases have also been discussed by Taşeli and coworkers [18,19].

The pseudospectral methods evaluate the eigenfunctions on a grid of points which coincide with the quadrature points for the weight function chosen. The diagonalization of the discrete matrix representative of the Hamiltonian of dimension $N^2$ gives $N$ eigenvalues of which a subset corresponds to the discrete eigenvalues for the problem. The spectral convergence of the eigenvalues refers to the exponential decrease of the error in the approximate eigenvalues versus $N$. Spectral convergence has been demonstrated recently by Lo and Shizgal [20] for several one dimensional problems. The present paper is a continuation of these earlier studies but we here consider a shift and scaling of the quadrature points which we demonstrate can accelerate the convergence.

Shizgal and coworkers [13,20,21] have demonstrated that rapid convergence of the eigenvalues of the Fokker–Planck equation can be obtained with a basis set defined by the equilibrium probability density as the weight function. The Fokker–Planck equation can be transformed to a Schrödinger equation with a potential such that the Hamiltonian belongs to the class of supersymmetric quantum mechanics for which the ground state is known [12]. Chen and Shizgal [10] and Lo and Shizgal [20] obtained rapid convergence of the eigenvalues of the Hamiltonian operator when the square of the ground-state eigenfunction is used for the weight function. Occasionally modifications of these weight functions are still required to improve convergence [10,20]. In most applications, such nonclassical basis sets were used. This method is referred to as the quadrature discretization method (QDM) since it is implemented as a pseudospectral (collocation) method. The QDM is generally based on quadrature points defined by nonclassical polynomials orthogonal with respect to a specific weight function.

There has been a long history of the application of numerical pseudospectral methods [22,23]. Shizgal [24] developed a pseudospectral method based on a Gaussian quadrature to accurately discretize the integral operator in the Boltzmann equation. By contrast, the calculation of the matrix elements of the Boltzmann collision operator in the basis set can lead to considerable round-off errors [25]. Shizgal and Blackmore [26] then applied this method to the solution of differential equations. The approach follows on previous works employing similar methods in neutron transport [27]. The QDM has been used to solve the time dependent Fokker–Planck equation [13,28], the Poisson equation [11], the advection-diffusion equation [29], and the Schrödinger equation [10,12,20].

An alternate method developed by Light and coworkers [14,30,31], which is referred to as the discrete variable representation (DVR), was originally based on the numerical evaluation of matrix elements of the potential in the Schrödinger equation [32,33]. If $V(x)$ is the potential in a one-dimensional Schrödinger equation, then the matrix elements of $V(x)$ can be determined with a Gaussian quadrature, that is,

$$V_{mn} = \int_a^b \phi_m(x) V(x) \phi_n(x)\, \mathrm{d}x \approx \sum_{k=1}^{N} \eta_k \phi_m(x_k) V(x_k) \phi_n(x_k), \tag{1}$$

where $\{\phi_n\}$ is a set of orthonormal basis functions, and $\{x_k\}$ and $\{\eta_k\}$ are appropriate sets of quadrature points and weights, respectively [34]. The DVR is also a pseudospectral method in which the solution is evaluated at a set of grid points analogous to the QDM. The DVR was thus introduced by Light et al. [30,31] and applied to several quantum problems [14,35–38].

We consider a set of polynomials $P_n(x)$ orthogonal with respect to a weight function $w(x)$,

$$\int_R w(x) P_m(x) P_n(x)\, \mathrm{d}x = \delta_{mn},$$

where $R$ denotes the domain for $x$. With $w_k = \eta_k w(x_k)$, there is a unitary transformation, $T_{kn} = \sqrt{w_k} P_{n-1}(x_k)$, between the representation of a function in a basis set (that is the coefficients $c_n$ in $\psi(x) = \sum_n c_n \phi_n(x)$ with $\phi_n(x) = \sqrt{w(x)} P_{n-1}(x)$) and the discrete representation, $\psi(x_k)$. The transformation of $V_{mn}$, Eq. 1, with $\mathbf{T}$ gives the diagonal representation of the potential in the discrete representation, that is, $V(x_k)$. Further details are provided in [12,13,28] and Sect. 2.

Thus the QDM was developed originally for kinetic theory problems whereas the DVR was introduced for the accurate evaluation of potential matrix elements. In Sect. 2, we briefly explain the variational principle and spectral convergence. Section 3 discusses the formulation of the pseudospectral method and the differences between QDM and DVR. Several applications are presented in Sects. 4–6 with discussions of results in 7.

## 2 Spectral convergence

The solution of the Schrödinger equation

$$H\psi = -\frac{\hbar^2}{2\mu} \frac{\mathrm{d}^2\psi}{\mathrm{d}x^2} + V\psi = E\psi,$$

is generally considered with the expansion of the eigenfunctions in a basis set,

$$\psi(x) \approx \sqrt{w(x)} \sum_{n=1}^{N} c_n P_{n-1}(x). \tag{2}$$

The matrix representation of the Hamiltonian in this basis set is $H_{mn} = (\hbar^2/2\mu)K_{mn} + V_{mn}$, where

$$K_{mn} = -\int_R \sqrt{w(x)}P_{m-1}(x)\frac{\mathrm{d}^2}{\mathrm{d}x^2}\left[\sqrt{w(x)}P_{n-1}(x)\right]\mathrm{d}x, \tag{3a}$$

$$V_{mn} = \int_R w(x)P_{m-1}(x)V(x)P_{n-1}(x)\,\mathrm{d}x. \tag{3b}$$

The expansion coefficients $c_n$ in Eq. 2 can be considered as linear variational parameters. The extremum of $\int_R \psi(x)H\psi(x)\,\mathrm{d}x/\int_R \psi(x)\psi(x)\,\mathrm{d}x$ with respect to $c_n$ is equivalent to the diagonalization of the finite matrix $H_{mn}$ [39]. Thus, we can refer to this basis set as the variational basis representation (VBR) as proposed by Light et al. [31]. The eigenvalue estimates converge monotonically to the exact eigenvalues from above. Spectral convergence refers to the exponential decrease of the coefficients $c_n$ versus $n$ as shown in Fig. 2 and in Fig. 6 of [20].

## 3 Pseudospectral method

Pseudospectral methods were popularized by researchers interested in the numerical solution of problems in fluid dynamics [22,23]. The set of polynomials orthogonal with respect to a chosen weight function, $w(x)$ can be generated with the algorithm as described elsewhere [27,40]. These polynomials define the quadrature points $x_k$ and weights $w_k$ for the quadrature rule

$$\int_R w(x)f(x)\,dx \approx \sum_{k=1}^{N} w_k f(x_k). \tag{4}$$

If the coefficients $c_n$ in Eq. 2 are evaluated with the quadrature rule in Eq. 4, the expansion of $\psi(x)$ is written as

$$\psi(x) \approx \sum_{k=1}^{N} I_k(x)\sqrt{\frac{w(x)}{w(x_k)}}\psi(x_k),$$

where the interpolating polynomial, $I_k(x)$, is given by

$$I_k(x) = w_k \sum_{n=1}^{N} P_{n-1}(x_k)P_{n-1}(x),$$

and $I_k(x_j) = \delta_{jk}$ satisfies the cardinality. The expansion of $\psi(x)$ in terms of normalized interpolating functions as basis functions was discussed by Baye and coworkers [15,17], and is referred to as a Lagrange mesh.

The QDM considers the symmetric kinetic energy matrix elements that results from an integration by parts, that is,

$$K_{mn} = \int_R \frac{\mathrm{d}}{\mathrm{d}x}\left[\sqrt{w(x)}P_{m-1}(x)\right]\frac{\mathrm{d}}{\mathrm{d}x}\left[\sqrt{w(x)}P_{n-1}(x)\right]\mathrm{d}x,$$

provided that the boundary term vanishes. After the derivatives are evaluated and one of the cross terms is integrated by parts, $K_{mn}$ can be written as

$$K_{mn} = \int_R w(x)P'_{m-1}(x)P'_{n-1}(x)\,\mathrm{d}x - \int_R w(x)P_{m-1}(x)\tilde{V}(x)P_{n-1}(x)\,\mathrm{d}x,$$

where

$$\tilde{V}(x) = \frac{1}{2}\frac{w''(x)}{w(x)} - \frac{1}{4}\left[\frac{w'(x)}{w(x)}\right]^2$$

is a reference potential [12]. The Hamiltonian matrix is therefore

$$H_{mn} = \frac{\hbar^2}{2\mu}\int_R w(x)P'_{m-1}(x)P'_{n-1}(x)\,\mathrm{d}x + \int_R w(x)P_{m-1}(x)\left[V(x) - \frac{\hbar^2}{2\mu}\tilde{V}(x)\right]P_{n-1}(x)\,\mathrm{d}x. \tag{5}$$

As shown elsewhere [10,12], the discrete representation of the Hamiltonian is obtained with $H_{mn}$ and the transformation $\mathbf{T}$ and we have that

$$H_{ij}^{\mathrm{QDM}} = \frac{\hbar^2}{2\mu}\sum_{k=1}^{N} D_{ki}D_{kj} + \left[V(x_i) - \frac{\hbar^2}{2\mu}\tilde{V}(x_i)\right]\delta_{ij}, \tag{6}$$

where

$$D_{ij} = \sqrt{w_i w_j}\sum_{n=1}^{N} P'_{n-1}(x_i)P_{n-1}(x_j),$$

is the discrete representation of the first derivative operator. Szalay [38] has provided explicit formulas for $D_{ij} = \int_R w(x)\mathcal{P}_i(x)\mathcal{P}'_j(x)\,\mathrm{d}x$ and $\sum_{k=1}^{N} D_{ki}D_{kj} = \int_R w(x)\mathcal{P}'_i(x)\mathcal{P}'_j(x)\,\mathrm{d}x$ where $\mathcal{P}_i(x) = w_i^{-1/2}I_i(x)$ (Table 2 of [38]).

For the QDM, the reference potential, $\tilde{V}(x)$, written in terms of the weight function forms an important aspect of the development. If $w(x)$ can be chosen such that $V(x) \equiv (\hbar^2/2\mu)\tilde{V}(x)$, the discrete representation of the Hamiltonian reduces to $H_{ij}^{\mathrm{QDM}} = (\hbar^2/2\mu)\sum_{k=1}^{N} D_{ki}D_{kj}$, and is calculated exactly with the quadrature. Thus, the QDM

preserves the variational aspects of the VBR. By contrast, applications with the DVR can lead to errors arising from the inexactness of the quadrature, Eq. 1, and "ghost" levels have been reported [41,42]. There is a class of Schrödinger equations that are isospectral with equivalent Fokker–Planck equations [12,43]. The eigenfunction of the Fokker–Planck equation with zero eigenvalue is the equilibrium distribution function which is known, $P_{\rm eq}(x) = \exp\left(-\int^x W(x')\,{\rm d}x'\right)$. For these problems, the ground-state of the Schrödinger equation is $\psi_0(x) = \sqrt{P_{\rm eq}(x)}$. The function $W$ is the superpotential in supersymmetric quantum mechanics [12,44]. If there is no convenient choice for $w(x)$ such that $V(x) = (\hbar^2/2\mu)\tilde{V}(x)$, one can choose a $w(x)$ so that $(\hbar^2/2\mu)\tilde{V}(x)$ is close to $V(x)$.

It has been shown [16] that scaling and translating of $x$ can often improve the convergence of the eigenvalues. The scaled and translated Hamiltonian is given by

$$H_{ij}^{\rm QDM} = \frac{\hbar^2}{2\mu}\frac{1}{s^2}\sum_{k=1}^{N} D_{ki}D_{kj} + \left[V(sx_i+b) - \frac{\hbar^2}{2\mu}\frac{1}{s^2}\tilde{V}(x_i)\right]\delta_{ij}, \tag{7}$$

where $x_i$ has been multiplied by the scaling factor $s$ and translated by $b$.

## 4 The vibrational states of the Morse oscillator

The Morse potential for $I_2$ has been well studied [8,17,20,45]. The potential is defined by

$$V_{\rm Morse}(x) = D_e\left[1-\exp(-\alpha(x-x_e))\right]^2 - D, \tag{8}$$

where $D_e = 0.0224$, $D = 0$, $\alpha = 0.9374$, $x_e = 0$, $\hbar^2 = 1$, $\mu = 119406$, and $x \in (-\infty, \infty)$, all in atomic units. The exact eigenvalues are given by

$$E_m^{\rm exact} = \frac{\hbar^2}{2\mu}\alpha^2\left(m+\frac{1}{2}\right)\left(\frac{2}{\alpha}\sqrt{\frac{2\mu}{\hbar^2}D_e} - \left(m+\frac{1}{2}\right)\right) - D, \tag{9}$$

for $0 \le m \le 77$. The ground state eigenfunction is

$$\psi_0^{\rm Morse}(x) = \exp\left[-\sqrt{\frac{2\mu}{\hbar^2}D_e}\left(x - x_e + \frac{\exp(-\alpha(x-x_e))}{\alpha}\right) + \frac{\alpha(x-x_e)}{2}\right].$$

The Morse potential belongs to the family of shape invariant potentials of supersymmetric quantum mechanics [44]. If the weight function for the polynomial expansion is chosen to be $w(x) = [\psi_0^{\rm Morse}(x)]^2$, the effective potential in Eq. 6 is simply $(\hbar^2/2\mu)\tilde{V}(x_i) = V_{\rm Morse}(x_i) - E_0$. With this choice of weight function, the discrete representation of the Hamiltonian, Eq. 6, reduces to $H_{ij}^{\rm QDM} = (\hbar^2/2\mu)\sum_{k=1}^{N} D_{ki}D_{kj} + E_0\delta_{ij}$.

With scaling $s$ and translation $b$, the QDM representation of the Hamiltonian is given by Eq. 7, where $V(sx_i + b) = V_{\text{Morse}}(sx_i + b)$. This scaling and translation of the grid points was not used in [20].

The QDM is almost always considered with nonclassical polynomials, whereas the DVR approach often uses classical bases (Fourier, Hermite, Laguerre, etc.). It is this different choice of basis set that distinguishes the two methods. Thus a typical DVR approach to this problem is to choose a classical polynomial basis such as Hermite polynomials. The DVR representation of the discrete Hamiltonian is

$$H_{ij}^{\text{Herm}} = \frac{\hbar^2}{2\mu}\frac{1}{s^2}K_{ij}^{\text{Herm}} + V_{\text{Morse}}(sx_i + b)\delta_{ij}, \tag{10a}$$

with the kinetic energy operator

$$K_{ij}^{\text{Herm}} = -\left\{\delta_{ij}\left[-\frac{2(N-1)}{3} - \frac{1}{2} + \frac{x_i^2}{3}\right] + (1-\delta_{ij})\left[\frac{1}{2} - \frac{2}{(x_i - x_j)^2}\right]\right\}. \tag{10b}$$

reported by Szalay [38]. Thus it is clear that the QDM and the DVR are pseudospectral methods of solution of the Schrödinger equation but are based on different weight functions and quadrature points. A comparison of the application of both methods to this system is presented in Sect. 7.

## 5 The vibrational states of $Ar_2$

The Cahill and Parsegian $Ar_2$ potential [46]

$$V(x) = a\exp(-bx)(1-cx) - \frac{d}{x^6 + ex^{-6}}, \tag{11}$$

where $x \in [0, \infty)$ is the radial coordinate in Å and $V(x)$ in eV. The parameters in Eq. 11 are $a = 1,720\,\text{eV}$, $b = 2.6920\,\text{Å}^{-1}$, $c = 0.2631\,\text{Å}^{-1}$, $d = 37.943\,\text{eV Å}^6$, $e = 177{,}588\,\text{Å}^{12}$, $\hbar^2 = 0.0041801588\,\text{eV u Å}^2$, and $\mu = 20\,\text{u}$. This potential has eight bound states. The weight function is chosen by approximating this potential with a Morse potential in Eq. 8 such that the $x$-intercept and the minimum of the well coincides with Eq. 11. We thus get the parameters $D_e = 0.01239309488\,\text{eV}$, $D = D_e$, $\alpha = 1.685967091\,\text{Å}^{-1}$, and $x_e = 3.761961562\,\text{Å}$. The weight function is thus $w(x) = [\psi_{\text{Morse}}(x)]^2$ defined on $x \in [0, \infty)$. With this weight function, the QDM representation of the Hamiltonian is given by Eq. 7, where $(\hbar^2/2\mu)\tilde{V}(x_i) = V_{\text{Morse}}(x_i) + D - \alpha\sqrt{D_e\hbar^2/2\mu} + (\hbar^2/2\mu)(\alpha^2/4)$.

For the DVR, the classical Laguerre polynomials defined on $x \in [0, \infty)$ and orthogonal with respect to $w(x) = x^2\exp(-x)$ are used. The Hamiltonian in the Laguerre basis is given by

$$H_{ij}^{\text{Lag}} = \frac{\hbar^2}{2\mu}\frac{1}{s^2}K_{ij}^{\text{Lag}} + V(sx_i + b)\delta_{ij}, \tag{12a}$$

where the discrete symmetric matrix representative of the kinetic energy is given by [15]

$$K_{ij}^{\mathrm{Lag}} = \begin{cases} 9/4x_i^2 + S_{ii} & \text{if } i = j, \\ (-1)^{i-j}[(3/2)(x_i x_j)^{-1/2}(x_i^{-1} + x_j^{-1}) + S_{ij}] & \text{if } i \neq j. \end{cases} \tag{12b}$$

and

$$S_{ij} = \sqrt{x_i x_j} \sum_{k=1, k\neq i,j}^{N} \frac{1}{x_k(x_k - x_i)(x_k - x_j)}. \tag{12c}$$

## 6 Woods–Saxon potential

As a third sample problem, we also consider the calculation of the bound states of the Woods–Saxon potential which is defined by

$$V(x) = \frac{u_0}{1+t} - \frac{u_0 t}{a_0(1+t)^2}$$

where $t = \exp((x - x_e)/a_0)$, $u_0 = -50$, $x_e = 7$, $a_0 = 0.6$, $\hbar^2 = 1$, $\mu = 0.5$, and $x \in [0, \infty)$. This potential has been considered by Simos [47] with an improved finite difference scheme, by Wang [48,49] using an improved Numerov method, and by Zakrzewski [50] using a power series method. Since this potential has a shape close to the square well potential

$$V_{\mathrm{sq}}(x) = \begin{cases} u_0 & \text{if } 0 \leq x < L, \\ 0 & \text{if } x \geq L, \end{cases}$$

with $L = 6.2$, we consider the square of the ground-state eigenfunction of $V_{\mathrm{sq}}(x)$ as the weight function, i.e. $w(x) = [\psi_0^{\mathrm{sq}}(x)]^2$, where

$$\psi_0^{\mathrm{sq}}(x) = \begin{cases} c_1 \sin(c_2 x) & \text{if } 0 \leq x < L, \\ \exp(c_3 x) & \text{if } x \geq L, \end{cases} \tag{13}$$

$c_1 = \exp(c_3 L)/\sin(c_2 L)$, $c_2 = \sqrt{\epsilon_0 - u_0}$, and $c_3 = -\sqrt{-\epsilon_0}$. The ground-state eigenvalue $\epsilon_0$ for $V_{\mathrm{sq}}(x)$ is the first root of the equation

$$\sqrt{\epsilon_0 - u_0}\cot(\sqrt{\epsilon_0 - u_0}L) = -\sqrt{-\epsilon_0},$$

or $\epsilon_0 = -49.75457960982555$. The QDM representation is given by Eq. 7, where $(\hbar^2/2\mu)\tilde{V}(x_i) = V_{\mathrm{sq}}(x_i) - \epsilon_0$.

## 7 Results and discussions

We have calculated the eigenvalues for the $I_2$ potential, Eq. 8, with the diagonalization of Eq. 7. The convergence of $E_{10}$ for three different discretizations is shown in Table 1. In the first column, the eigenvalue estimate obtained with the QDM with no translation or scaling of the quadrature points converges monotonically to within seven significant figures of the exact value. The underlined portions of the estimates in the table show the converged values to five significant figures. In the second column of Table 1, we show the improved convergence with scaling $s = 1.05$ although it is no longer monotonic from above. The eigenvalue estimate exhibits a minimum versus $N$ at $N = 15$. The scaling $s$ and translation $b$ changes the weight function to $[\psi_0^{\text{Morse}}((x-b)/s)]^2$ so that $V(x)-(\hbar^2/2\mu)\tilde{V}(x)$ is no longer a constant, and the second integral in Eq. 5 cannot be evaluated exactly by quadrature. Hence, the QDM representative of the Hamiltonian in Eq. 7 is not equivalent to the basis set representation and the variational principle no longer holds. The eigenvalues calculated with the diagonalization of the discrete Hamiltonian in the scaled Hermite basis set, Eq. 10a, is shown in the third column of Table 1. The eigenvalues converge nonmonotonically as well and slower than the QDM results.

Figure 1 shows the convergence of $E_1$, $E_{10}$, $E_{30}$, and $E_{50}$ for the Morse potential given by Eq. 8. The negative of the relative error, defined by

$$\epsilon_m(N) = \log \left| \frac{E_m^{(N)} - E_m^{\text{exact}}}{E_m^{\text{exact}}} \right|,$$

represents approximately the number of significant figures for $E_m^{(N)}$. The exact eigenvalues $E_m^{\text{exact}}$ are given by Eq. 9. The QDM results for $E_1$ without scaling shown in

**Table 1** Convergence of $10^3 E_{10}$ for the $I_2$ Morse potential

| $N$ | (a) | (b) | (c) |
|---|---|---|---|
| 11 | 6.397074 | 6.432646 | 9.203165 |
| 12 | 5.929980 | 5.749709 | 6.515301 |
| 13 | 5.731211 | 5.634366 | 5.285059 |
| 14 | 5.653056 | 5.625372 | 5.229673 |
| 15 | 5.629265 | 5.623171 | 5.177875 |
| 16 | 5.624138 | 5.623269 | 5.524050 |
| 17 | 5.623357 | 5.623259 | 5.464870 |
| 18 | 5.623268 | 5.623260 | 5.615021 |
| 19 | 5.623260 | | 5.619430 |
| 20 | | | 5.623601 |
| 21 | | | 5.622067 |
| 22 | | | 5.623292 |
| 23 | | | 5.623252 |
| 24 | | | 5.623235 |
| 25 | | | 5.623258 |
| 26 | | | 5.623257 |
| 27 | | | 5.623260 |
| 28 | | | 5.623259 |
| 29 | | | 5.623260 |

Numbers are underlined when 5 significant figures are achieved

(a) QDM $s = 1$, $b = 0$;
(b) QDM $s = 1.05$, $b = 0$;
(c) Hermite $s = 0.14$, $b = 0$

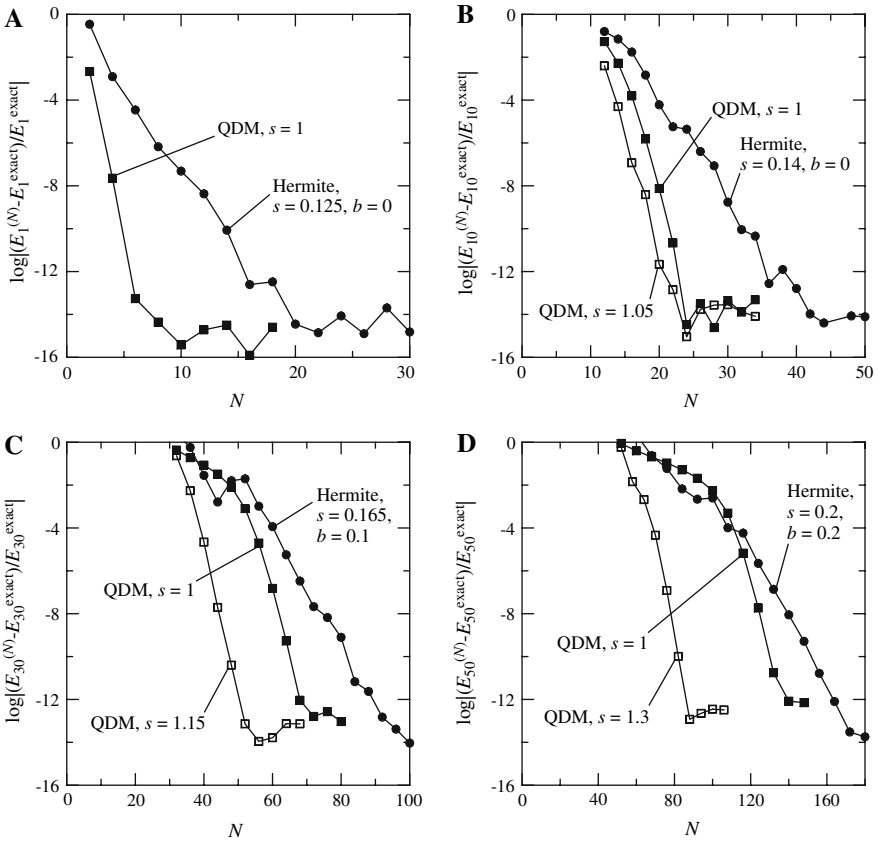


**Fig. 1** Variation of $\log|(E_m^{(N)} - E_m^{\text{exact}})/E_m^{\text{exact}}|$ versus the number of quadrature points $N$ for the $I_2$ Morse potential. QDM: Eq. 7 with $b = (1-s)x_1$; Hermite: Eq. 10. (**a**): $m = 1$; (**b**): $m = 10$; (**c**): $m = 30$; (**d**): $m = 50$

Fig. 1a converge much faster than the results with DVR with scaled Hermite polynomials. In Fig. 1b–d, the convergence of the eigenvalues $E_{10}$, $E_{30}$, and $E_{50}$ evaluated with the QDM is also much faster than the DVR results with Hermite polynomials. In order to capture the behaviour of the eigenfunctions for the higher states which are more loosely bound, the scale factor introduced for QDM serves to expand the computational domain. The scaling of the QDM is particularly important for $E_{50}$. The translation of the QDM grid, $b = (1-s)x_1$, is chosen to keep the lowest grid point unchanged while the length of the computational domain is scaled by $s$, which is optimized by trial and error. The results with Hermite polynomials are also optimized with the values of $s$ and $b$ by trial and error.

The fast rate of convergence for the QDM is anticipated because the $m$th eigenfunction $\psi_m(x)$ is expanded in polynomials orthogonal with respect to the weight function $w(x) = [\psi_0(x)]^2$. The first excited state, $\psi_1(x)$, is the simplest one to represent in the basis set generated with this weight function, and thus we obtain the very rapid convergence of $E_1^{(N)}$, as shown in Fig. 1a.

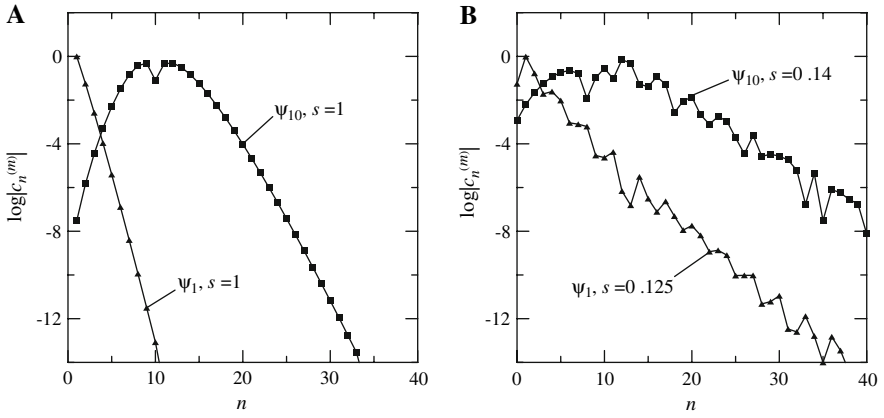


**Fig. 2** Variation of the expansion coefficients $c_n^{(m)}$ versus $n$ for $\psi_m(x)$ of the $I_2$ system for $m = 1$ and 10 for both QDM and Hermite. (**a**) QDM with $b = 0$. (**b**) Hermite with $b = 0$

In Fig. 2a we show the variation of the coefficients $c_n^{(m)}$ for the $m$th eigenfunction versus $n$ for $m = 1$ (triangles) and $m = 10$ (squares). The rapid exponential decrease of $c_n^{(1)}$ versus $n$ is an illustration of spectral convergence. The QDM yields diagonally dominant matrix representations in the polynomial basis set as discussed previously by Lo and Shizgal [20] and thus gives the rapid spectral convergence shown in Fig. 1.

The variation of the coefficients $c_n^{(m)}$ versus $n$ for $m = 1$ and 10 in the Hermite expansion

$$\psi_m(y) \approx \exp\left(-\frac{1}{2}\left[\frac{y-b}{s}\right]^2\right)\sum_{n=1}^{N} c_n^{(m)} Q_{n-1}^{(s,b)}(y), \tag{14}$$

where $y = sx + b$ is the scaled and translated coordinate, is shown in Fig. 2b with triangles and squares, respectively. In Eq. 14, $Q_n^{(s,b)}(y) = \nu_n H_n((y-b)/s)$ are the scaled and translated Hermite polynomials normalized by the constants $\nu_n$. Spectral convergence is also confirmed, but the rate of decrease of $c_n^{(m)}$ is slower than with the QDM. For $m = 10$, the spectral convergence refers to the exponential decrease in the expansion coefficients $c_n^{(10)}$ versus $n$ for $n \gtrsim 10$ beyond the maxima shown in Fig. 2.

Figure 3 shows the convergence of the eigenvalues $E_0$, $E_3$, $E_5$, and $E_7$ for $Ar_2$. The potential supports 8 bound states. The exact eigenvalues, $E_m^{\text{exact}}$, used for calculating the errors are evaluated in multiple precision with a higher order method and are assumed to be correct to at least 20 significant digits. In Fig. 3, we show that the QDM discretization gives a very rapid convergence rate for the four eigenvalues when appropriate scalings are used. The results for the scaled and translated Laguerre expansion are also shown in Fig. 3. Since the eigenfunctions are concentrated in the region of the potential well, in order to improve the convergence of the Laguerre expansion a translation of the grid points is essential. This changes the weight function to $w(y) = ((y-b)/s)^2 \exp(-(y-b)/s)$ and the computational domain to $y \in [b, \infty)$. This translation redistributes the Laguerre quadrature points concentrated near $x = 0$

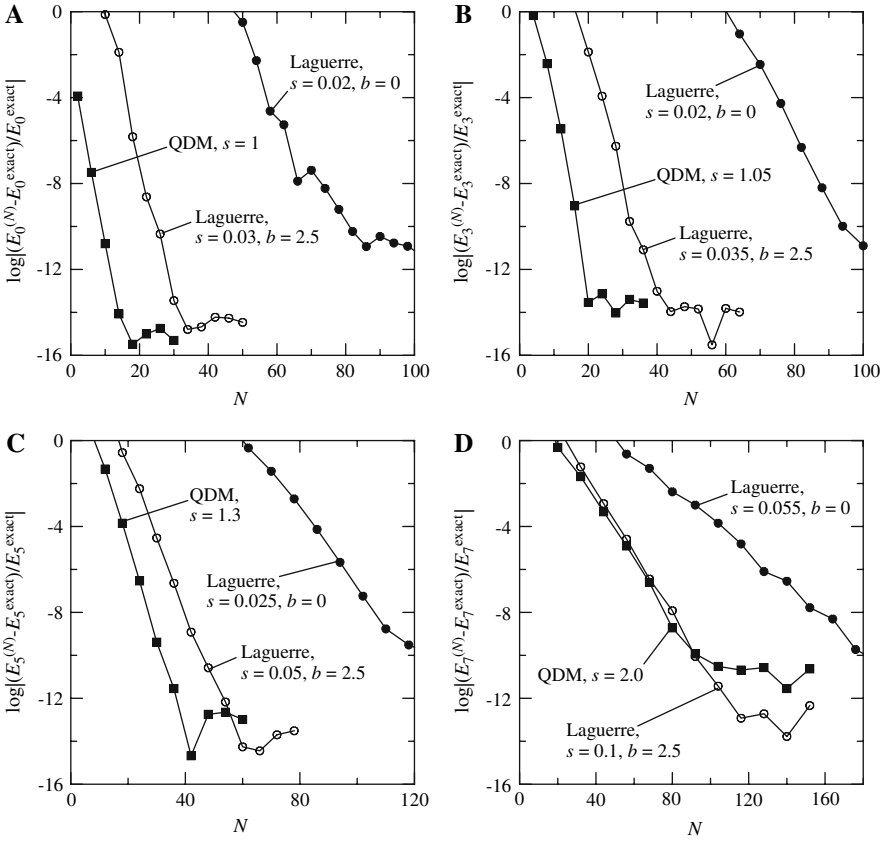


**Fig. 3** Variation of $\log|(E_m^{(N)} - E_m^{\text{exact}})/E_m^{\text{exact}}|$ versus the number of quadrature points $N$ for the $Ar_2$ Cahill and Parsegian potential. QDM: Eq. 7 with $b = (1 - s)x_1$; Laguerre: Eq. 12. (**a**) $m = 0$; (**b**) $m = 3$; (**c**) $m = 5$; (**d**) $m = 7$

to the region of the potential well. The value of $b$ for each state must be chosen appropriately such that the domain truncation error incurred by neglecting the contribution from $[0, b)$ is less than machine precision and the convergence rate of the eigenvalue is nearly optimized.

For the Woods–Saxon potential, we use the ground state eigenfunction, Eq. 13, of a square well potential as the weight function which generates the basis set and quadrature points used in the QDM. The diagonalization of the matrix representative of the Hamiltonian given by Eq. 7 gives approximate eigenvalues for the Woods–Saxon potential. Because the imposed boundary conditions, $\psi(0) = \psi(\infty) = 0$, are the same for both the square well potential and the Woods–Saxon potential, no translation of grid points is required, i.e. $b = 0$. To evaluate the accuracy of the approximate eigenvalues we compare these with the exact numerical values reported by Ledoux [51]. In Fig. 4, the values of $s$ for the curves labeled with the open circles were chosen so that $\epsilon_m(N) \approx -6$ and remains more or less constant with increasing $N$. We suspect that the minimum error of $10^{-6}$ which does not decrease with an

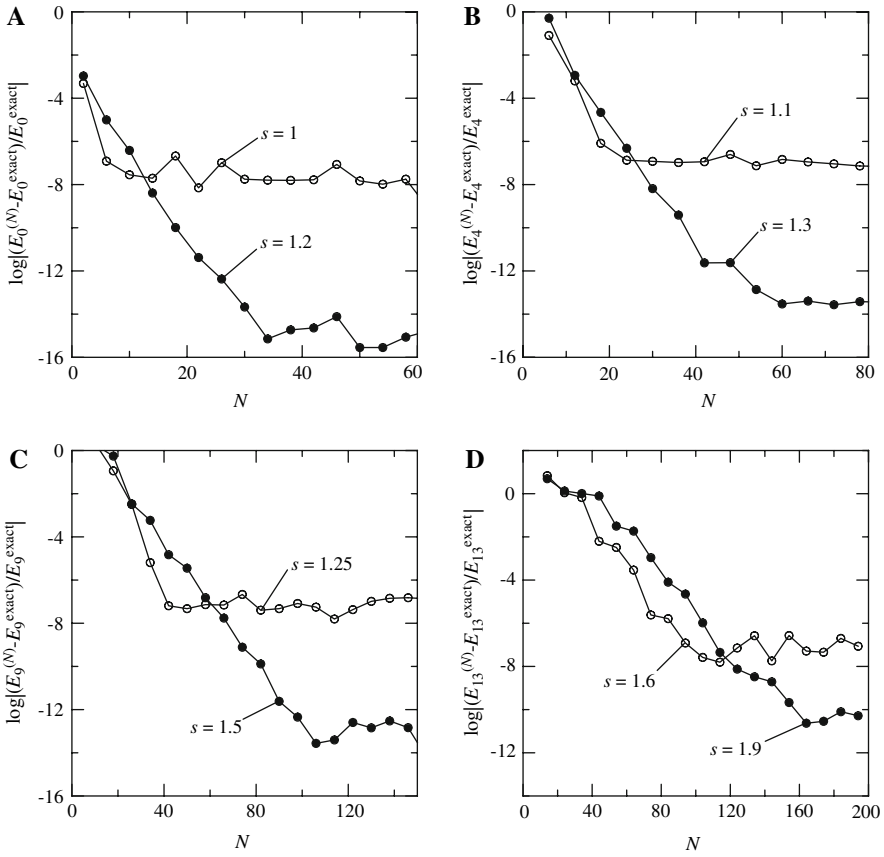


**Fig. 4** Variation of $\log|(E_m^{(N)} - E_m^{\text{exact}})/E_m^{\text{exact}}|$ versus the number of quadrature points $N$ for the Woods–Saxon potential by QDM. (**a**): $m = 0$; (**b**): $m = 4$; (**c**): $m = 9$; (**d**): $m = 13$

increase in $N$ arises from the subtraction of $(\hbar^2/2\mu)\tilde{V}(x)$, which is not continuous. If larger values of $s$ are chosen (filled circles), the accuracy of the eigenvalue estimates is improved to machine precision.

## 8 Summary

The quadrature discretization method (QDM) was originally developed to solve the time dependent Boltzmann and Fokker–Planck equations for the kinetic theory problems [12,13,21,24,26,28]. This motivated the concept of developing nonclassical basis sets for different problems based on weight functions that were associated with the equilibrium solution which is the ground state eigenfunction. The spectral convergence of this large class of eigenvalue problems was found to be very rapid. The DVR was developed from the need to calculate potential energy matrix elements numerically and quadrature methods were adopted, analogous to applications of the Boltzmann

equation [24,28]. The numerical implementation of the QDM and the DVR is with a pseudospectral approach that was developed by workers in fluid mechanics [22,23]. In the present paper, we have demonstrated that the convergence of the vibrational states of $Ar_2$ and $I_2$ is accelerated with the appropriate choice of the basis set modified by scaling and translation of the coordinate. The convergence with Hermite or Laguerre basis functions which are often the basis sets of choice for many applications of the DVR is generally much slower.

**Acknowledgements** This research is supported by a grant to BDS from the Natural Sciences and Engineering Research Council of Canada. BDS is grateful to Dr. Phillipe Maisonobe and Dr. Alain Pumir for their hospitality at the University of Nice.

## References

1. T.E. Simos, J. Math. Chem. **40**, 305 (2006)
2. Z. Kalogiratou, Th. Monovasilis, T.E. Simos, J. Math. Chem. **37**, 271 (2005)
3. Z. Kalogiratou, T.E. Simos, J. Math. Chem. **31**, 211 (2002)
4. Z.A. Anastassi, T.E. Simos, J. Math. Chem. **41**, 79 (2007)
5. Th. Monovasilis, Z. Kalogiratou, T.E. Simos, J. Math. Chem. **40**, 257 (2006)
6. Th. Monovasilis, T.E. Simos, Comput. Mater. Sci. **38**, 526 (2007)
7. F.M. Fernández, Q. Ma, R.H. Tipping, Phys. Rev. A **40**, 6149 (1989)
8. M. Braun, S.A. Sofianos, D.G. Papageorgiou, I.E. Lagaris, J. Comput. Phys. **126**, 315 (1996)
9. M.R.M. Witwit, J.P. Killingbeck, Can. J. Phys. **73**, 632 (1995)
10. H. Chen, B.D. Shizgal, J. Math. Chem. **24**, 321 (1998)
11. H. Chen, B.D. Shizgal, J. Comput. Appl. Math. **136**, 17 (2001)
12. B.D. Shizgal, H. Chen, J. Chem. Phys. **104**, 4137 (1996)
13. B.D. Shizgal, H. Chen, J. Chem. Phys. **107**, 8051 (1997)
14. J.C. Light, T. Carrington, Adv. Chem. Phys. **114**, 263 (2000)
15. D. Baye, P.H. Heenen, J. Phys. A: Math. Gen. **19**, 2041 (1986)
16. D. Baye, M. Hesse, M. Vincke, Phys. Rev. E **65**, 026701 (2002)
17. D. Baye, M. Vincke, Phys. Rev. E **59**, 7195 (1999)
18. H. Taşeli, M. Bahar Erseçen, J. Math. Chem. **34**, 177 (2003)
19. H. Taşeli, H. Alıcı, J. Math. Chem. **41**, 407 (2007)
20. J. Lo, B.D. Shizgal, J. Chem. Phys. **125**, 194108 (2006)
21. B. Shizgal, J. Chem. Phys. **70**, 1948 (1979)
22. C. Canuto, M.Y. Hussaini, A. Quarteroni, T.A. Zang, *Spectral Methods in Fluid Dynamics* (Springer-Verlag, New York, 1988)
23. R. Peyret, *Spectral Methods for Incompressible Viscous Flow* (Springer-Verlag, New York, 2002)
24. B. Shizgal, J. Comput. Phys. **41**, 3091 (1981)
25. M.J. Lindenfeld, B. Shizgal, Chem. Phys. **41**, 81 (1979)
26. B. Shizgal, R. Blackmore, J. Comput. Phys. **55**, 313 (1984)
27. R.D.M. Garcia, Prog. Nucl. Energy **35**, 249 (1999)
28. R. Blackmore, B.D. Shizgal, Phys. Rev. A **31**, 1855 (1985)
29. B.D. Shizgal, Comput. Fluids **31**, 825 (2002)
30. J.V. Lill, G.A. Parker, J.C. Light, Chem. Phys. Lett. **89**, 483 (1982)
31. J.C. Light, I.P. Hamilton, J.V. Lill, J. Chem. Phys. **82**, 1400 (1985)
32. D.O. Harris, G.G. Engerholm, W.D. Gwinn, J. Chem. Phys. **43**, 1515 (1965)
33. A.S. Dickinson, P.R. Certain, J. Chem. Phys. **49**, 4209 (1968)
34. P.J. Davis, P. Rabinowitz, *Methods of Numerical Integration*, 2nd edn. (Academic Press, New York, 1984)
35. J. Echave, D.C. Clary, Chem. Phys. Lett. **190**, 225 (1992)
36. H. Karabulut, E.L. Sibert, J. Phys. B: At. Mol. Opt. Phys. **30**, L513 (1997)
37. B.I. Schneider, N. Nygaard, J. Phys. Chem. A **106**, 10773 (2002)
38. V. Szalay, J. Chem. Phys. **99**, 1978 (1993)
39. S.T. Epstein, *The Variational Method in Quantum Chemistry* (Academic Press, New York, 1974)

40. W. Gautschi, *Orthogonal Polynomials: Computation and Approximation* (Oxford, New York, 2004)
41. H. Wei, J. Chem. Phys. **106**, 6885 (1997)
42. K. Willner, O. Dulieu, F. Masnou-Seeuws, J. Chem. Phys. **120**, 548 (2004)
43. H. Risken, *The Fokker–Planck Equation* (Springer-Verlag, New York, 1984)
44. R. Dutt, A. Khare, U. Sukhatme, Am. J. Phys. **56**, 163 (1988)
45. D.A. Mazziotti, J. Chem. Phys. **117**, 2455 (2002)
46. K. Cahill, V.A. Parsegian, J. Chem. Phys. **121**, 10839 (2004)
47. T.E. Simos, Appl. Math. Comput. **106**, 245 (1999)
48. Z. Wang, Y. Ge, Y. Dai, D. Zhao, Comput. Phys. Commun. **160**, 23 (2004)
49. Z. Wang, Comput. Phys. Commun. **167**, 1 (2005)
50. A.J. Zakrzewski, Comput. Phys. Commun. **175**, 397 (2006)
51. V. Ledoux, M. Rizea, L. Ixaru, G. Vanden Berghe, M. Van Daele, Comput. Phys. Commun. **175**, 424 (2006)